electronics

MDPI

Article

Performance Analysis of Multihop Underground Magnetic Induction Communication

Mariam Ishtiaq and Seung-Hoon Hwang *

Division of Electronics and Electrical Engineering, Dongguk University, Seoul 04620, Korea; mariam.ishtiaq@gmail.com

* Correspondence: shwang@dongguk.edu; Tel.: +82-2-2260-3994

Abstract: Magnetic induction (MI) is a promising solution for realizing wireless underground sensor networks (WUSNs) for many applications such as smart agriculture, surveillance, and environmental monitoring. In this study, a practical deployment model for a multihop MI-WUSN was developed, and its end-to-end performance was evaluated in terms of the signal-to-noise ratio, channel capacity, and bit error rate. We considered a multihop MI-WUSN and evaluated its end-to-end statistical performance for two scenarios pertaining to the hop state: (1) independent and identical distribution (IID) and (2) independent and non-identical distribution (INID). We derived analytical expressions for the performance evaluation and analysis of both scenarios by varying the number of hops and channel conditions. Our extensive numerical results show that asymptotic performance bounds can be obtained for the IID of hops. An analysis of the INID of hops yielded practical results that can facilitate decisive optimisation trade-offs and that can help reduce the system design overhead.

Keywords: wireless underground sensor network (WUSN); magnetic induction (MI); underground communication; decode-and-forward (DF); end-to-end; multihop; relay; system performance; bit error rate (BER)

Citation: Ishtiaq, M.; Hwang, S.-H. Performance Analysis of Multihop Underground Magnetic Induction Communication. *Electronics* **2021**, *10*, 1255. https://doi.org/10.3390/electronics10111255

Academic Editor: Rameez Asif

Received: 16 March 2021
Accepted: 21 May 2021
Published: 24 May 2021

1. Introduction

Underground communication has recently gained considerable attention owing to its wide range of applications including seismic and climate change monitoring, smart agriculture, mining, infrastructure monitoring, industrial Internet of Underground Things (IoUT) and border patrol [1–5]. Existing well-established communication protocols for above-the-ground communication cannot be directly modeled for underground communication because of the dynamic nature of the channel and the unpredictability of its characteristics such as temperature, humidity and composition, which directly influence signal propagation [2,3,6]. Consequently, many different communication techniques have been investigated, such as those involving electromagnetic (EM) waves [7], acoustic waves [8] and magnetic induction (MI) [9]. A detailed overview of different underground communication techniques and their applications is presented in [10]. Figure 1 shows simplistic underground communication systems based on EM, acoustic and MI protocols, covering a transmission distance r between a source (Tx) and a sink (Rx). The EM wave technique [11,12] is used for underground communication when the antenna size is large, while acoustic waves are not suitable for underground media owing to limitations associated with possible vibrations [13]. MI is a promising physical layer technique for wireless underground sensor networks (WUSNs) and it offers the following benefits.

- It allows inter-medium communication between air and soil, between soil and water and between air and water owing to the nearly constant magnetic permeability of air and water [14].
- It renders the channel response predictable because of easy penetration and negligible multipath fading [15].

- It offers low cost and design efficiency because of the simplistic hardware (a coil) involved. [14,16].

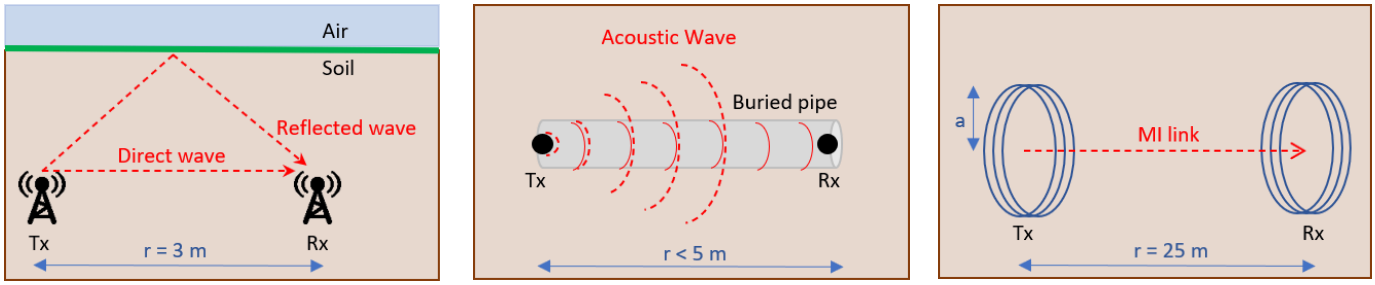

(**a**) (**b**) (**c**)

Figure 1. Simple wireless underground communication systems based on (**a**) electromagnetic waves, (**b**) acoustic waves and (**c**) magnetic induction (MI).

These benefits can be enhanced by using multihop MI transmission, which is an effective way to divide the communication link from the source to the destination into several hops using relays. Relays have been used to achieve a myriad goals. In [17], the magnetic field detector with high sensitivity was used to achieve a high communication range, and in [18] pulse powered magnetic induction (PPMI) was used to reduce the path loss and thereby increase the communication distance.

In multihop communication, relays are primarily used for reducing signal attenuation in long-range communication and for deriving cooperative diversity benefits [19]. Passive relays, which are merely repeaters with small coils that use minimal energy and are cost efficient, were used for MI waveguides in [14] to increase the communication range. The downside to using waveguides is the limited bandwidth they offer. To extend the communication range using relays and without additional power consumption by the WUSN, [20] proposed an optimal relay position related to the system configuration. To extend the range further and gain a bandwidth advantage, [21] used active relays (with the capability to perform some operation on the received signal). Active relays have two major operation modes: amplify and forward (AF) and decode and forward (DF). In the AF mode, the signal received at the non-regenerative relay is amplified (along with noise) and then forwarded. By contrast, the DF mode decodes the signal at the generative relay and then forwards it. Active relaying is an energy-consuming protocol, and therefore it has been used in parallel with simultaneous wireless information and power transfer schemes [22]. Apart from range extension, MI relays have been studied for various other purposes. Some of them are as follows:

- Diversity gain by using relay selection protocols [23] and network orientation [24]
- Mitigation of interference in the form of crosstalk in MI-based multiple-input multiple-output systems [25]
- Noise modeling [21]
- Network throughput improvement by using an optimal relay position [26]
- Determination of outage probability and analysis of connectivity [27]

Despite all the studies on MI relays, some assumptions made in previous studies restrict the practicality of the solution. For example, in the range extension techniques proposed in [21] and the data rate improvement technique presented in [28], all the nodes are assumed to be deployed in a homogeneous conductive environment (soil and tunnel, respectively), with constant properties over space and time. Such an assumption poses practical limitations on system design and analysis since any sudden change in the propagation characteristics renders the extraction of the desired signal at the receiver end inefficient. The change of the channel state has been discussed in earlier works such as [29,30]. Most recent works such as [31–33] also analyse non-homogeneous channel conditions. To the best of our knowledge, there has been no study on multihop relay-based MI-WUSNs that

has investigated independent and non-identical channel states between hops and their impact on the system performance. The important features of this work are as follows:

- A basic point-to-point underground communication model involving MI was extended to develop a multihop underground MI-based communication system.
- A mathematical model was developed for evaluating the performance of the proposed MI communication system under the following assumptions.
    a. Statistically independent and identical distribution (IID) of channel states between hops
    b. Statistically independent and non-identical distribution (INID) of channel states between hops
- While earlier work in this domain has been based on an asymptotic analysis, we evaluated the performance by using different system parameters and validated its efficacy with extensive numerical analysis.

Our evaluations showed that if a communication system is designed for fixed channel state information (CSI) under the IID assumption for the hop state, the corresponding overestimated model can cause performance overhead when the communication system is practically deployed. Accordingly, current solutions should be updated to account for this change in the channel state on all hops, by providing an adaptive and scalable solution instead of a theoretical model based on impractical assumptions.

The rest of this paper is organised as follows. Section 2 presents the traditional MI communication system model for point-to-point communication and its extension to multihop MI communication. Section 3 details a mathematical model for analysing single-hop and multihop MI-WUSNs for IID and INID cases. Section 4 presents numerical results of the proposed model, and finally, Section 5 concludes this paper.

2. Underground MI Communication System

In this section, we develop a point-to-point MI communication model and evaluate the performance of an MI communication system for single-hop communication. Further, we extend the model to multihop communication and discuss system parameters.

2.1. Single-Hop MI Communication Model

A simple schematic of an MI communication model comprising a source node (Tx) and a transmitter node (Rx) separated by distance r, over which an MI communication link is established, is shown in Figure 2. Both nodes have identical configurations; namely, each node is a coil of diameter d, and serve as magnetic antennas. We considered a standard American Wire Gauge, for which the resistance per unit length, R_0, of the loops could vary between 2×10^{-4} and $3\ \Omega/\mathrm{m}$ [14].

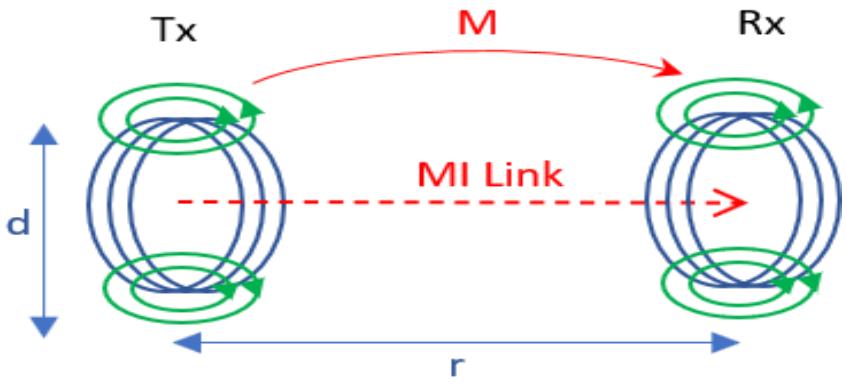

Figure 2. MI communication model for single hop communication.

In single-hop communication, the transmitter directly induces a voltage in the receiver circuit. The underlying principle of MI communication is that when a time-varying electric signal is induced in the transmitter coil, a time-varying magnetic field is generated around the coil. The coupling of this magnetic field with the neighbouring coil (relay or receiver) induces a voltage in the coil, thereby establishing a communication link between the two coils. This communication link is said to be established on the basis of mutual induction (M) between the two coils (or nodes), and it can be expressed as [14,20].

$$M = \mu\pi N_k^2 \frac{a_k^4}{2r^3}. \tag{1}$$

Here, N_k is the number of turns of coil k, a_k denotes the radius of the coil, and r is the internode distance. The impedance Z of the circuit is given by

$$Z = R + j\omega L + \frac{1}{j\omega C}, \tag{2}$$

where $\omega = 2\pi f_0$ denotes the angular frequency of the circuit for operation at the resonant frequency f_0. For a resonant circuit, the inductance L and capacitance C are related as

$$LC = \frac{1}{\omega^2}. \tag{3}$$

The capacitor is designed to satisfy the resonance condition [20]

$$j\omega L + \frac{1}{j\omega C} = 0 \tag{4}$$

The received power P_r and transmit power P_t can be evaluated as [14]

$$\frac{P_r}{P_t} = \frac{Z \cdot U_K^2}{\left(Z + Z_K + \acute{Z_K}\right)^2} \cdot \frac{Z_{K-1} + \acute{Z_{K-1}}}{U_{K-1}^2}, \tag{5}$$

where Z is the load impedance. The subscript K denotes the receiver while $K-1$ is used for transmitter. U_K and U_{K-1} are voltages and Z_K and Z_{K-1} are the impedances of receiver and transmitter, respectively. In the next section, we develop a multihop communication system on the basis of this single-hop communication model.

2.2. Multihop MI Communication Model

In this study, we developed an MI-WUSN by using a linear system model in a one-dimensional region $\mathcal{R}$. To model an MI communication system, let us consider K nodes such that $\mathcal{K} = \{1, 2, 3, \ldots, K\}$ is a set of nodes aligned in $\mathcal{R} = [0, R]$, and let there be (K–2) relay nodes between the transmitter and receiver. The K nodes are arranged along $\mathcal{R}$, establishing i equidistant hops such that $h_i \in \{1, 2, \ldots, H\}$, with $H = K - 1$. This path can be defined as an ordered set of nodes, that is, $\mathcal{H} = 0 \leq h \leq H$, and each hop can be represented by $h_i = |\mathcal{H}|$. The position of each node k, where $k = 1, 2, 3, \ldots, K$, is denoted by x_k. The source node is at $x_1 = 0$ while the sink node is at $x_K = R$. The distance between any two nodes k and $k + 1$ is $r_{(k,k+1)}$. For equidistant nodes, we have $r_{(1,2)} = r_{(2,3)} = \ldots = r_{(K-1,K)}$. The sink node is connected to a gateway node that transmits data to the above-ground channel for processing. A detailed visualisation of this notational convention is presented in Figure 3.

In contrast to the traditional mesh networks [34] that depend on a routing technique to relay messages, the proposed linear network topology offers an inherently simplified routing mechanism. Each node in the linear network [26] propagates the message to the next node since communication is based on the strength of the mutual induction between two consecutive nodes. A mesh network topology would be a costly alternative to the suggested linear topology in terms of high deployment effort as well as low network

lifetime, especially for challenging underground environment. To demonstrate how multihop communication can enhance the overall system robustness, we first develop an MI communication system based on the above strategy and then present a methodology for analytically evaluating the communication system's performance. We also analyse the impact of different channel states between hops for a multihop MI-WUSN.

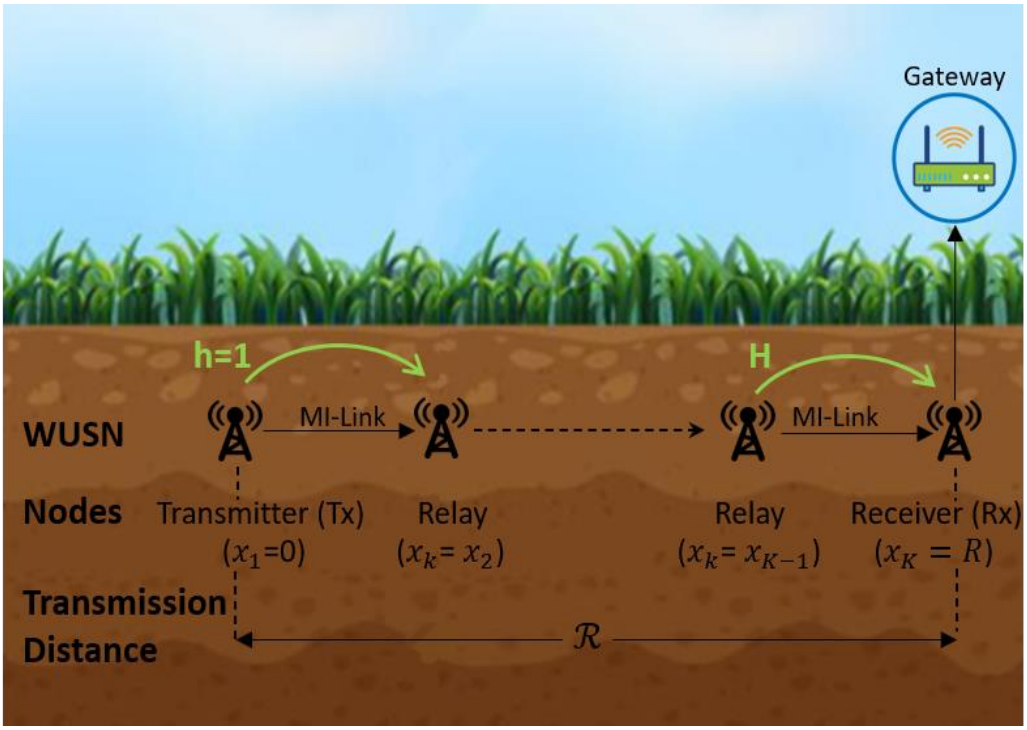

Figure 3. Proposed multihop MI communication system.

3. Performance Analysis

In this section, we propose an MI-WUSN evaluation methodology for single-hop and multihop systems. Table 1 shows a summary of how MI-WUSNs have been studied most recently in comparison to this work to analyse the system performance in dynamic channel conditions.

Table 1. A summary of comparison between this work and other MI-WUSNs.

Comparison	[14]	[15]	[26]	Proposed Work
Environment	Underground, soil medium	Underground, underwater	Underwater	Underground, soil medium
Communication medium	Homogeneous	Homogeneous and non-homogeneous	Non-homogeneous (Ocean water)	Homogeneous and non-homogeneous
Number of hops	Multihop	Single hop	Multihop	Single hop and multihop
System parameters	Path loss, BER, Bandwidth	Multipath Fading, Penetration efficiency, Attenuation loss	Number of relays, Throughput	SNR, Channel capacity, BER
Communication range	≈10 m	0.3 m	≈25 m	25 m

The literature presented in Table 1 gives an insight into different approaches towards MI-WUSN solutions for dynamic and extreme channel conditions like underground and underwater. Table 1 clearly indicates that the proposed work is unique and comprehensive, and a higher communication range can be achieved using the given methodology compared to the other work in literature. We present a novel system performance evaluation methodology in terms of three key performance indicators (KPIs), i.e., signal-to-noise ratio (SNR), channel capacity and bit error rate (BER). Following the performance evaluation of point-to-point or single hop communication using MI-WUSN, the impact of static and varying channel state between multiple hops will be evaluated. With varying channel state, the deviation in system performance metrics will be studied compared to the asymptotic bounds offered by statis channel conditions. The associated trade-offs will also be analysed and discussed.

3.1. Single-Hop MI Communication Model

From Figure 2, a statistical model of a single-hop MI communication system can be developed by defining the source node (Tx) as node 1 and the destination node (Rx) as node K. We wish to evaluate the probabilistic system performance by assuming constant channel conditions over r. One of the fundamental evaluation parameters of any wireless communication system is the average signal-to-noise ratio (average SNR), defined as the statistical average of the received signal over the probability density function (PDF) of fading. Thus, the average error rate performance can be evaluated by averaging the instantaneous error rate over the SNR distribution [35]. For a single hop h from Tx to Rx, the SNR γ for a single bit is given by

$$\gamma = \frac{E_b}{N_0}, \tag{6}$$

where E_b is the mean energy per transmitted bit and N_0 is the power spectral density of thermal noise. Since the underground channel is subject to fading, the received signal power is attenuated by the fading amplitude, denoted by α, which is a random variable whose PDF is conditioned on the nature of fading. The mean square value of the fading amplitude $\overline{\alpha^2}$ is used to define the average SNR per bit, $\overline{\gamma}$, given by

$$\overline{\gamma} = \alpha^2 \frac{E_b}{N_0}. \tag{7}$$

The SNR, measured in dB, at the receiver can be defined as

$$SNR = P_t - PL_{MI} - P_n, \tag{8}$$

where P_t and P_n denote the transmit power and noise power in dBm, respectively. A generalised form of the path loss PL_{MI} in dBm can be written as [14].

$$PL_{MI} = -10 \log \frac{P_r}{P_t}. \tag{9}$$

After the SNR (dB) is evaluated from (8), it is first converted to a power ratio in linear scale as:

$$SNR_{linear} = 10^{(SNR/10)} \tag{10}$$

System performance metrics such as the channel capacity and bit error rate (BER) can be obtained using (10). The channel capacity C for system bandwidth W can be obtained using the Shannon capacity theorem:

$$C = W \, log_2(1 + SNR_{linear}). \tag{11}$$

Further, we compare the BER performance of two modulation schemes, namely binary amplitude shift keying (2ASK) [18] and binary phase shift keying (2PSK) [36], by using the following expressions:

$$BER_{2ASK} = \frac{1}{2} erfc \sqrt{\frac{SNR_{linear}}{4}}. \quad (12)$$

$$BER_{2PSK} = \frac{1}{2} erfc \sqrt{SNR_{linear}}. \quad (13)$$

The BER is an important statistical performance measure for a channel as it is used to design error control schemes. This statistic can be used to determine the channel behaviour and therefore has vital significance in varying channel conditions. A target symbol error rate (SER) of $\approx 10^{-3}$ has been used in [29] for MI-WUSN deployed in underground monitoring applications for varying CSI. Since an underground channel has a dynamic state, this research aims to evaluate the variation of a multihop communication system's performance in terms of the SNR, channel capacity and BER, for a dynamic channel state between hops, in contrast to the commonly used research assumption of an identical channel state between hops. The average bit error probability (BEP) E_h over a single hop h can be defined as

$$E_h = E_k(\gamma_k), \quad (14)$$

where $E_k(\gamma)$ is the average BEP at the receiver node k in the underground channel. For H hops such that $h \in H$, we devise a realistic end-to-end performance evaluation strategy in the next section. To extend the single-hop system to a multihop communication model, we considered the following two scenarios.

1. A generic multihop scenario where all hops are statistically independent and identical
2. A multihop scenario where hops are statistically independent but not identical, which is practical for modeling underground communication

3.2. Multihop MI Communication with Statistically Independent and Identical Hops (Balanced Hops)

First, we develop a system model with IID of channel states between hops. To analyse a basic multihop communication model and its performance, we assume the basic multihop case with two hops ($H = 2,\ K = 3$). If h_1 and h_2 are the first and second hops, we obtain errors at the sink for the following two cases.

Case 1: h_1 is correctly received but h_2 has an error.

Case 2: h_1 has an error but h_2 is correctly received.

Let E_h be the probability that a bit is received in error at hop h. Then, the probability that h_1 is correctly received can be defined using (14) as $(1 - E_{h1}(\gamma_{h1}))$, and the probability that h_2 is correctly received can be defined by $(1 - E_{h2}(\gamma_{h2}))$. For multiple hops i, these definitions can be generalised to $(1 - E_{i-1})$ and $(1 - E_i)$, respectively. Thus, the error probability at the *ith* hop (for *two* statistically independent hops) can be given by the joint recursive probability [37]

$$E_{i=2}(\gamma_{i-1}, \gamma_i) = (1 - E_{i-1}(\gamma_{i-1}))E_i(\gamma_i) + (1 - E_i(\gamma_i))E_{i-1}(\gamma_{i-1}). \quad (15)$$

Let us denote the end-to-end BER in a multihop network with IID of channel characteristics between hops by E_H. By using the analogy employed in (15), we obtain

$$E_H = E(H)(1 - E_{H-1}) + E_{H-1}(1 - E(H)). \quad (16)$$

By rearranging this equation, we can obtain

$$E_H = E(H) + E_{H-1}(1 - 2E(H)). \quad (17)$$

By using the substitution method that is used to solve linear ordinary differential equations, we can determine E_{H-1} from (17):

$$E_{H-1} = E(H) + E_{H-2}(1 - 2E(H)). \tag{18}$$

Substituting the expression for E_{H-1} in (18) into the recurrent relation (17), we obtain

$$E_H = E(H) + E(H)(1 - 2E(H)) + E_{H-2}(1 - 2E(H))^2. \tag{19}$$

Expanding this series over H hops yields

$$E_H = E(H) + E(H)(1 - 2E(H)) + \ldots + E_1(1 - 2E(H))^H. \tag{20}$$

Under the assumption of IID of all hops, the following equality holds true:

$$E_1 = E_2 = \ldots = E_i, \forall i \in 1, 2, \ldots, H. \tag{21}$$

Using (21) and applying summation to (20), we have the final BEP of an end-to-end multihop network under the assumption of IID of channel states between hops:

$$E_H = \sum_{i=0}^{H-1} E_i(1 - 2E_i)^i \tag{22}$$

According to [38], an upper bound for this end-to-end BER is

$$E_H = 1 - (1 - E_i)^H \tag{23}$$

3.3. Multihop MI Communication with Statistically Independent Non-Identical Hops (Unbalanced Hops)

In the practical realisation of MI-WUSNs, when static nodes are buried underground, the fading amplitude can vary despite the well-controlled conditions, owing to unforeseen circumstances such as sudden seismic changes, ground water penetration, and interference. Even the assumption of equidistant nodes does not hold over time because of the possibility of the position and orientation of the deployed static antenna changing because of, say, pressure caused by factors such as growth of plant roots or interaction with subsurface animals such as rabbits. Therefore, one of the most critical aspects of underground communication is establishing long-range communication in the heterogeneous underground environment. For such non-identical hops, the error probability of each hop E_h for $h \in \{1, 2, \ldots, K-1\}$ depends on the state of the underground channel. The underground channel can be considered to be slowly fading [35], and hence, the instantaneous CSI varies across hops, with the variation depending on the fading amplitude (7); this variation causes the SNR γ_i to vary. In this case, consecutive links cannot be characterised by the same BEP (E_i). This error probability is a function of the SNR and is bounded by the link with the weakest SNR [39], that is, $\gamma_{i=2} = min\{\gamma_1, \gamma_2\}$. The end-to-end SNR γ_{e2e} can then be written as

$$\gamma_{e2e} \approx \min_{i=1,\ldots,H} \gamma_i \tag{24}$$

For a multihop communication model, (24) is a tight approximation for determining the end-to-end system SNR. The end-to-end channel capacity of a relay channel is also bounded by (24), so applying the max-flow min-cut theorem [40], the upper bound for channel capacity of a multihop relay based MI-WUSN can be given as:

$$C_{e2e} = \min_{i=1,\ldots,H} C_i(\gamma_i). \tag{25}$$

If there are INID states between hops, the error probability of each hop is different and (21) becomes an inequality. Using the multinomial theorem [41], we can express the term $(1-2E(H))^H$ in (20) as the recurrence relation

$$(1-2E(H))^H = \prod_{j=1}^{H}(1-2E_j). \tag{26}$$

Therefore, substituting (26) in (20), we can obtain the end-to-end BER for the INID of multihop in an MI-WUSN as

$$E_H = \sum_{i=1}^{H}\left(E_i \prod_{j=i+1}^{H}(1-2E_j)\right) \tag{27}$$

A closed-form upper-bounded expression for (27) is presented in [38] as

$$E_H = 1 - \prod_{i=1}^{H}(1-2E_i) \tag{28}$$

We can also see that (27) converges to (22), provided the initial condition E_i remains constant for all hops under condition (21):

$$E_H = \sum_{i=1}^{H}\left(E_i \prod_{j=i+1}^{H}(1-2E_j)\right) = \sum_{i=0}^{H-1} E_i(1-2E_i)^i. \tag{29}$$

This expression proves the validity of both (22) and (27) for the IID and INID of hop states in an MI-WUSN, respectively.

4. Numerical Results

In this section, we summarise the results of the analytical model proposed in Section 3 for an MI-WUSN system's performance evaluation. We present the end-to-end system performance for single-hop and multihop MI-WUSNs under assumptions of similar and different channel states determined by the noise power. A numerical analysis was performed using the system model presented in Section 2 and the system performance analysis methodology proposed in Section 3. The default values for the evaluation parameters listed in Table 2 have been adapted from [14] since they have been extensively tested and used in experiments [29] and testbeds [36] alike. All the coils used in the proposed system, i.e., transmitter, relay and receiver, have the same size and dimension for the sake of consistency. To overcome the proximity effect of the coils placed in a close vicinity, a small operational frequency of 10 MHz is used with small number of turns, i.e., 5. Though, this limits the achievable system bandwidth to 2 kHz, this is enough for the practical sensing and monitoring applications like disaster or breach detection in mines or borders, and smart farming applications to sense the water content. Processing on the data can be done on cloud using the external gateways connected at the receiver to maximize the battery lifetime of the overall system, since battery replacement or node re-deployment are challenging and costly operations for MI-WUSN.

We analyse the system using the approach shown in Figure 4.

Table 2. Parameters used for evaluating the wireless underground MI sensor network system's performance.

Parameter	Value
Operational frequency, f	10 MHz
Transmission distance, $\mathcal{R}$	25 m
Number of nodes, k (with K–2 relays)	0–12
Number of turns, N	5
Coil radius, a	0.15 m
Resistance per unit length, R_0	0.01
System Bandwidth, W	2000 Hz
Noise power, P_n	$P_{n(min)} = -103$ dBm, $P_{n(max)} = -83$ dBm
Magnetic Constant, μ_0	$4\pi \times 10^{-7}$ H/m

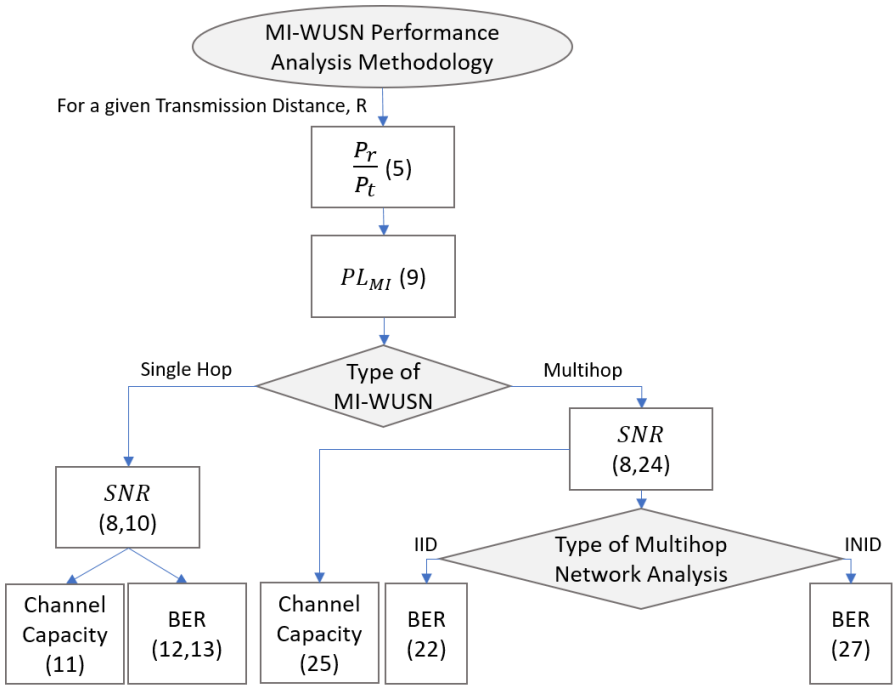

Figure 4. Performance analysis methodology of multihop underground magnetic induction communication system in terms of SNR, channel capacity and BER. For a given transmission distance, performance evaluation has been carried out for three types of networks: (1) single hop, (2) multihop with independent and identical distribution (IID) of hop states, and (3) multihop with independent and non-identical distribution (INID) of hop states.

4.1. Single-Hop MI-WUSN Performance

Figure 5 shows the result of a performance analysis of point-to-point communication performed with the single-hop model of Section 3.1. The results in Figure 5a,b can be recreated using (8) and (11), respectively. Figure 5c is based on (12) and (13). Figure 5a shows that the SNR for high noise power (−83 dBm) is lower than that for low noise power (−103 dBm) and decreases with increasing transmission distance. The channel capacity in Figure 5b is lower for high noise power and decreases with increasing transmission distance. The BER performance in Figure 5c shows that binary phase-shift keying (BPSK) is a better modulation scheme than 2ASK for both low and high noise scenarios. Accordingly, further analysis in this study was performed for BPSK modulation.

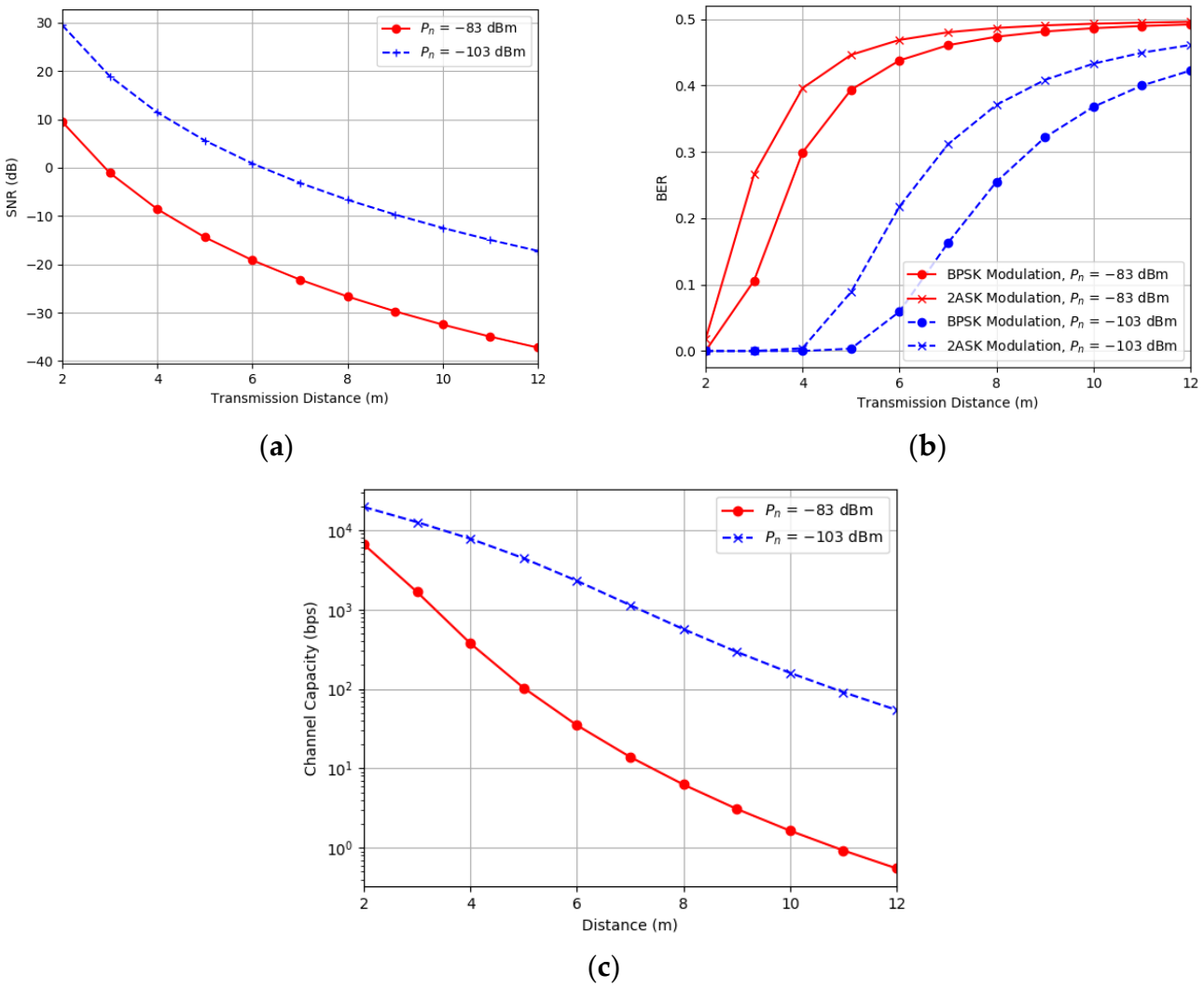

Figure 5. Single-hop underground MI communication performance. The panels show the variation in the (**a**) signal-to-noise ratio (SNR (dB)), (**b**) channel capacity (bps) and (**c**) bit error rate (BER) over the transmission distance at low noise power ($P_n = -103$ dBm) and high noise power ($P_n = -83\ dBm$) for the binary phase shift keying and binary amplitude shift keying modulation schemes.

To emphasise the significance of an MI-based underground communication system beyond asymptotic analysis based on static channel conditions, Figure 6 shows the variation of the achievable BER with noise in the link for a given SNR. It can be clearly seen that for the achievement of a reference BER of 0.25, internode distances of around 3, 5 and 8 m are required for high noise power (−83 dBm), average noise power (−93 dBm) and low noise power (−103 dBm), respectively. Alternatively, the optimal internode distance can increase from 3 m to 8 m as the noise decreases from −83 dBm to −103 dBm. We can therefore deduce that the results of an earlier work based on an asymptotic analysis for MI-WUSN design in which the channel properties were considered to be constant are not applicable to multihop analysis, since a variation in the any of the links can change the system performance. This implies that system design for best/worst case scenarios is not practically feasible so smart design optimizations need to be analysed.

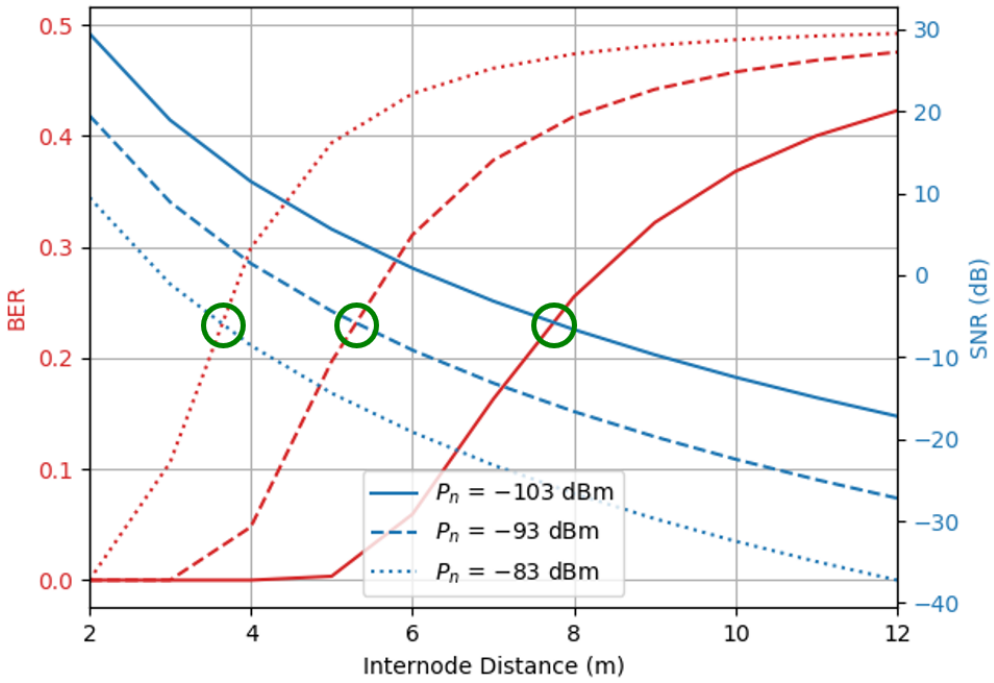

Figure 6. Variation of the SNR and BER with the internode distance at a fixed high noise power ($P_n = -83$ dBm), the average noise power ($P_n = -93$ dBm) and a low noise power ($P_n = -103$ dBm).

4.2. Multihop MI-WUSN Performance for IID of Hops

We evaluated the performance of multihop communication under the assumption of the IID of channel states between equidistant hops (Section 3.2) and by using the evaluation parameters in Table 2. Figure 7a shows the variation of the SNR with the number of hops under IID for different values of the noise power. Evidently, for a fixed transmission distance of 25 m, the SNR improves with an increase in the number of intermediate relays. For constant conditions under the IID assumptions, all the results show similar trends. Figure 7b shows the variation of the channel capacity for different noise powers. For a given value of noise, if the internode distance is large (the case of two relays), the channel capacity remains low. For the improvement of the network channel capacity, the number of hops can be increased. For a higher noise value (−83 dBm), the capacity gain remains relatively low even for a large number of relays (10 relays). The BER performance in Figure 7c shows a similar trend. For a fixed transmission distance, the BER performance improves with an increase in the number of hops. This performance improvement is greater for low noise values compared with high noise values. From Figure 7b,c, we can infer that there is a trade-off between the achievable BER and the system channel capacity when defining the optimal number of hops for a given transmission distance. The curves in Figure 7 show a constant variation trend owing to the initial assumption of the IID of channel states between hops. This analysis can therefore provide asymptotic bounds for end-to-end system performance. The next section presents a practical analysis in which the variation of the channel state between hops was considered.

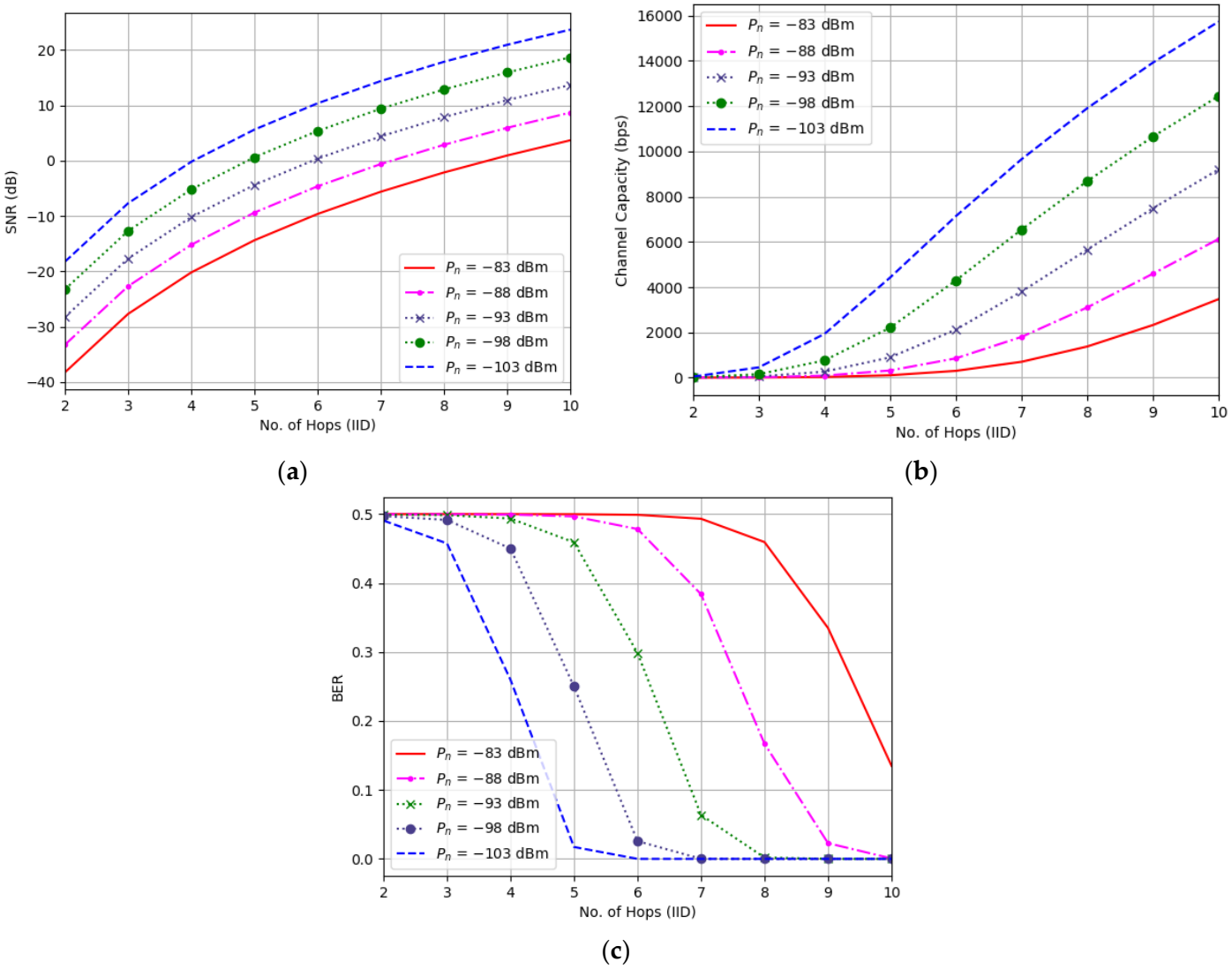

Figure 7. Multihop underground MI communication system's performance with IID of channel states between hops. The panels show the variation of the (**a**) SNR (dB), (**b**) channel capacity (bps) and (**c**) BER with the number of hops under different noise conditions.

4.3. Multihop MI-WUSN Performance for INID of Hops

To analyse the impact of the INID of the hop states in the practical deployment of an underground MI communication system, we first evaluated the variation of the end-to-end BEP with the SNR for the dual-hop scenario. For the unbalanced case, we considered that the SNR for the second hop was twice that of the first hop, that is, $\gamma_2 = 2\gamma_1$. For this analysis, we used (28) to model a multihop system with the INID of hop states. Evaluation results for the dual-hop BER are shown in Figure 8. Clearly, in the case of unbalanced hops, the performance varies, unlike the balanced hop scenario. Figure 8a shows that as the noise power increases in the dual-hop system, the BER performance is degraded. This is opposite to the trend in Figure 8b, where the BER performance improves with increasing SNR.

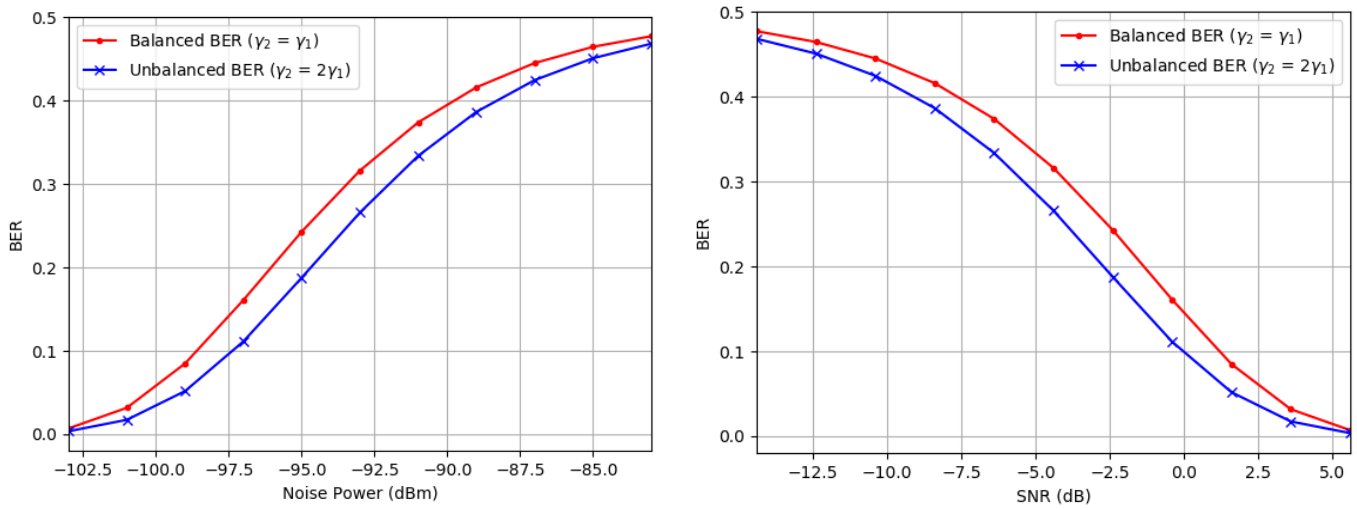

Figure 8. Variation in the BER for balanced ($\gamma_2 = \gamma_1$) and unbalanced ($\gamma_2 = 2\gamma_1$) dual-hop scenarios: plots of (**a**) BER vs. Noise Power ($P_n(dBm)$) and (**b**) BER vs. SNR.

Next, we extended this dual-hop analysis to the multihop scenario for the INID of hop states. For the analysis of the different channel states between consecutive hops as done in Section 3.3, there can be an infinite number of possibilities, which makes this analysis of NP hard complexity. To simplify this analysis and obtain meaningful results, we started from a given noise power P_n at the first hop and considered the following three scenarios in the analysis.

1. Increase/decrease of 0.5 dBm noise power at each hop
2. Increase/decrease of 1 dBm noise power at each hop
3. Increase/decrease of 1 dBm noise power after two hops

The resulting graphs in Figure 9 show the average end-to-end SNR, channel capacity and BER performance across a multihop network in which the first hop is subject to an average noise power of -93 dBm.

The average SNR increases with the number of hops in the network in Figure 9a. This gap in system performance is not large when the deviation across hops is smaller. This behaviour can be observed in cases when there is an increase/decrease of 0.5 dBm at each hop or 1 dBm after 2 hops in Figure 9a–c. Furthermore, the rate of increase rises sharply as the state between consecutive hops changes by a greater margin; in other words, the greater the deviation across consecutive hops, the more the expected decrease in the SNR. The channel capacity in Figure 9b and the BER in Figure 9c show similar trends. It can therefore be concluded that the more the deviation of successive hop states, the more the deviation in the system performance, unlike the asymptotic model. The BER performance for the proposed INID cases also shows that a higher BER for a greater deviation can be achieved by using a greater number of hops. This observation is highlighted in Figure 9c. Once again, the need to achieve a trade-off between the number of relays and the expected system performance becomes vital for the practical deployment.

The impact of the variation of the channel characteristics on the system performance is also shown in Figure 10, where hop 1 is characterized by either high (-83 dBm) or low (-103 dBm) noise power. The variation of this initial noise power across successive hops defines the end-to-end system performance. If the first hop is characterised by low noise, an increase of 1 dBm noise after two hops corresponds to the best end-to-end SNR performance in Figure 10a, the maximum channel capacity in Figure 10b, and the best BER performance in Figure 10c. The reverse also holds true for high noise at hop 1: after every two hops, the noise power decreases by 1 dBm. This decrease in noise corresponds

to the lowest performance of all evaluated cases, that is, for the SNR in Figure 10a, the channel capacity in Figure 10b, and the BER in Figure 10c. Figure 10 also indicates that for worse channel conditions at hop 1, represented by -83 dBm noise power that decreases over consecutive hops, high channel state variation across hops gives better performance, and vice versa. Alternatively, for good channel conditions at hop 1 (-103 dBm noise power), that worsen progressively over consecutive hops, lowest variation gives best overall system performance. This result is also consistent with (24) and (25) that bound the minimum system performance of a multihop MI-WUSN by the link with highest noise. On the contrary, if we compare the two possible states of hop 1 characterized by best and worst-case scenarios, the gap in system performance is large. This gap emphasizes the significance of accounting for deviation in channel state for practical system design.

From the results in Section 4.3, it is evident that end-to-end multihop communication performance is significantly influenced by the channel state between hops. Consequently, the assumption of identical hops may be useful only for simplifying system modeling, not for the practical deployment and analysis of the underground MI communication system. Therefore, the assumption of the IID of hops is impractical for the practical deployment of MI-WUSNs.

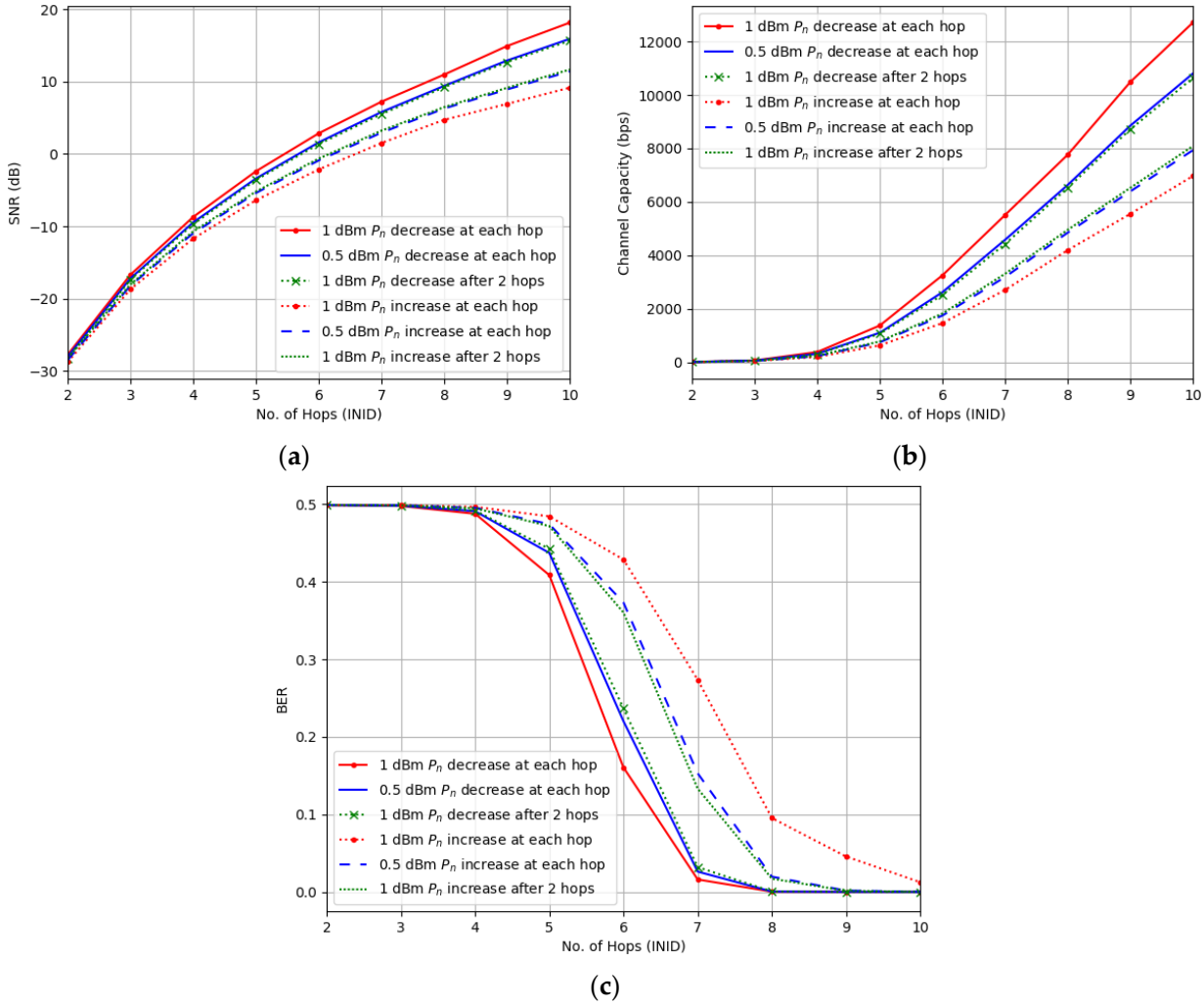

Figure 9. Multihop underground MI communication system's performance for INID of channel states between hops, with hop 1 subject to an average noise power of $P_n = -93$ dBm. The panels show the variation of the (**a**) SNR (dB), (**b**) channel capacity (bps) and (**c**) BER with the noise power across hops.

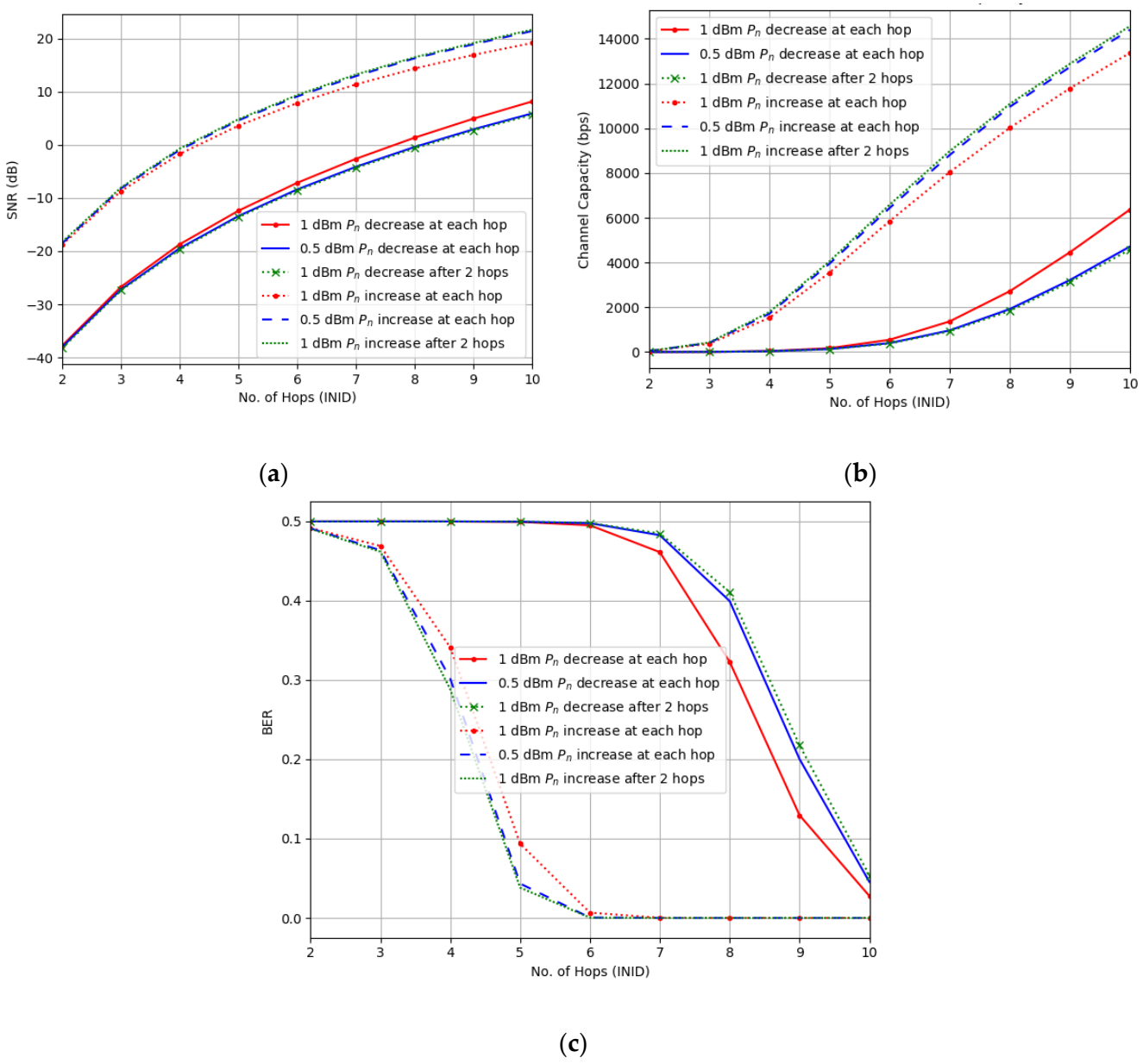

Figure 10. Multihop underground MI communication system's performance for INID of channel states between hops. Decreasing noise scenarios across hops were considered for high noise power ($P_n = -83$ dBm) at hop 1, and increasing noise scenarios across hops were considered for low noise power ($P_n = -103$ dBm) at hop 1. The panels show the variation of the (**a**) SNR (dB), (**b**) channel capacity (bps) and (**c**) BER with the noise power across hops.

5. Conclusions

In this paper, we have formulated a performance evaluation methodology for MI-WUSN using SNR, channel capacity and BER. We first studied the single hop communication model and concluded that system performance is directly dependent on the transmission distance for any given channel state. For instance, at high noise power, a shorter communication distance makes desirable system performance achievable and vice versa. Next, we present the end-to-end performance evaluation of a multihop MI-WUSN for a constant (IID) and changing (INID) channel state between hops. We derived analytical expressions for evaluating both scenarios and verified our hypothesis through extensive evaluations. Our results show that the assumption of the IID of hop states is impractical for an underground channel owing to the channel's inherently dynamic nature. For multihop MI-WUSN, more relays correspond to better performance irrespective of the channel

conditions due to stronger magnetic coupling. However, a trade-off should be achieved between the deployment cost of more relays and the required system performance. The system evaluation showed that with an increase in the number of links characterised by a low average SNR, the end-to-end BER increases while the overall system performance deteriorates. The more the deviation of channel state across successive hops is, the more the deviation in the system performance is observed.

Our analysis is general and can be easily extended to any channel model (such as the Rayleigh, Rice, and AWGN models) by adding the corresponding channel fading parameters. In the absence of any reported work on precise channel state modeling for underground communication in the context of multihop MI-WUSNs, our work provides an analytical model that can be used to study the performance of end-to-end MI-WUSNs for a time-varying underground channel. Furthermore, our results show that a margin for unexpected performance degradation should always be considered when modeling a practical MI-WUSN, because of the unpredictable underground channel state, which cannot be assumed to remain constant over space and time.

In the future, if packet error rate is to be analysed, higher order modulation and detection schemes would have to be employed using the approach proposed in this work. This is also applicable to computing the end-to-end delay of the relay channel which is dependent on parameters like the choice of relay scheme (AF or DF), SNR, the required BER and the decoding scheme applied at relay (DF) or destination (AF). Our work provides the foundation for such extensions.

Author Contributions: M.I. and S.-H.H. contributed to the main idea of this research. M.I. performed the numerical evaluation. M.I. and S.-H.H. contributed to the writing of this article. This research activity was planned and executed under the supervision of S.-H.H. Both authors have read and agreed to the published version of the manuscript.

Funding: This research received no external funding.

Conflicts of Interest: The authors declare no conflict of interest.

References

1. Kisseleff, S.; Akyildiz, I.F.; Gerstacker, W.H. Survey on Advances in Magnetic Induction-Based Wireless Underground Sensor Networks. *IEEE Internet Things J.* **2018**, *5*, 4843–4856. [CrossRef]
2. Huang, H.; Shi, J.; Wang, F.; Zhang, D.; Zhang, D. Theoretical and Experimental Studies on the Signal Propagation in Soil for Wireless Underground Sensor Networks. *Sensors* **2020**, *20*, 2580. [CrossRef]
3. Zungeru, A.M.; Chuma, J.; Mangwala, M.; Sigweni, B.; Matsebe, O. Signal Propagation and Analysis in Wireless Underground Sensor Networks. *Int. J. Eng. Res. Afr.* **2019**, *41*, 60–78. [CrossRef]
4. Sinha, R.S.; Wei, Y.; Hwang, S.-H. A survey on LPWA technology: LoRa and NB-IoT. *ICT Express* **2017**, *3*, 14–21. [CrossRef]
5. See, C.H.; Horoshenkov, K.V.; Abd-Alhameed, R.A.; Hu, Y.F.; Tait, S.J. A Low Power Wireless Sensor Network for Gully Pot Monitoring in Urban Catchments. *IEEE Sens. J.* **2012**, *12*, 1545–1553. [CrossRef]
6. Akyildiz, I.F.; Sun, Z.; Vuran, M.C. Signal propagation techniques for wireless underground communication networks. *Phys. Commun.* **2009**, *2*, 167–183. [CrossRef]
7. Elleithy, A.; Liu, G.; Elrashidi, A. Underground Wireless Sensor Network Communication Using Electromagnetic Waves Resonates at 2.5 GHz. *J. Wirel. Netw. Commun.* **2012**, *2*, 158–167. [CrossRef]
8. Yang, S.; Baltaji, O.; Singer, A.C.; Hashash, Y.M.A. Development of an Underground Through-Soil Wireless Acoustic Communication System. *IEEE Wirel. Commun.* **2020**, *27*, 154–161. [CrossRef]
9. Sun, Z.; Akyildiz, I. Key Communication Techniques for Underground Sensor Networks. *Found. Trends® Netw.* **2012**, *5*, 283–420.
10. Saeed, N.; Alouini, M.; Al-Naffouri, T.Y. Toward the Internet of Underground Things: A Systematic Survey. *IEEE Commun. Surv. Tutor.* **2019**, *21*, 3443–3466. [CrossRef]
11. Sun, Z.; Akyildiz, I.F. Underground Wireless Communication Using Magnetic Induction. In Proceedings of the 2009 IEEE International Conference on Communications, Dresden, Germany, 14–18 June 2009; pp. 1–5.
12. See, C.H.; Abd-Alhameed, R.A.; Atojoko, A.A.; McEwan, N.J.; Excell, P.S. Link Budget Maximization for a Mobile-Band Subsurface Wireless Sensor in Challenging Water Utility Environments. *IEEE Trans. Ind. Electron.* **2018**, *65*, 616–625. [CrossRef]
13. Salam, A.; Vuran, M.C.; Irmak, S. A Statistical Impulse Response Model Based on Empirical Characterization of Wireless Underground Channels. *IEEE Trans. Wirel. Commun.* **2020**, *19*, 5966–5981. [CrossRef]
14. Sun, Z.; Akyildiz, I.F. Magnetic Induction Communications for Wireless Underground Sensor Networks. *IEEE Trans. Antennas Propag.* **2010**, *58*, 2426–2435. [CrossRef]

15. Guo, H. Performance Analysis of Near-Field Magnetic Induction Communication in Extreme Environments. *Prog. Electromagn. Res.* **2020**, *90*, 77–83. [CrossRef]
16. Silva, A.R.; Moghaddam, M. Design and Implementation of Low-Power and Mid-Range Magnetic-Induction-Based Wireless Underground Sensor Networks. *IEEE Trans. Instrum. Meas.* **2016**, *65*, 821–835. [CrossRef]
17. Hott, M.; Hoeher, P.A.; Reinecke, S.F. Magnetic Communication Using High-Sensitivity Magnetic Field Detectors. *Sensors* **2019**, *19*, 3415. [CrossRef] [PubMed]
18. Zungeru, A.M.; Ezea, H.; Katende, J. Pulsed power system for wireless underground sensor networks. In Proceedings of the 2016 Third International Conference on Electrical, Electronics, Computer Engineering and their Applications (EECEA), Beirut, Lebanon, 21–23 April 2016; pp. 126–132.
19. Chakrabarti, A.; Sabharwal, A.; Aazhang, B. Fundamental Limits and Practical Implementation. Available online: https://www.semanticscholar.org/paper/Fundamental-Limits-and-Practical-Implementation-Chakrabarti-Sabharwal/7589ae6e303fc4820771a63a1def6289d60ac4f0 (accessed on 6 November 2020).
20. Qiao, G.; Muzzammil, M.; Ahmed, N.; Ullah, I. Experimental Investigation of Optimal Relay Position for Magneto-Inductive Wireless Sensor Networks. *Sensors* **2020**, *20*, 2720. [CrossRef]
21. Kisseleff, S.; Sackenreuter, B.; Akyildiz, I.F.; Gerstacker, W. On capacity of active relaying in magnetic induction based wireless underground sensor networks. In Proceedings of the 2015 IEEE International Conference on Communications (ICC), London, UK, 8–12 June 2015; pp. 6541–6546.
22. Asiedu, D.K.P.; Lee, H.; Lee, K. Simultaneous Wireless Information and Power Transfer for Decode-and-Forward Multihop Relay Systems in Energy-Constrained IoT Networks. *IEEE Internet Things J.* **2019**, *6*, 9413–9426. [CrossRef]
23. Kisseleff, S.; Akyildiz, I.F.; Gerstacker, W.H. Magnetic Induction-Based Simultaneous Wireless Information and Power Transfer for Single Information and Multiple Power Receivers. *IEEE Trans. Commun.* **2017**, *65*, 1396–1410. [CrossRef]
24. Dumphart, G.; Slottke, E.; Wittneben, A. Magneto-inductive passive relaying in arbitrarily arranged networks. In Proceedings of the 2017 IEEE International Conference on Communications (ICC), Paris, France, 21–25 May 2017; pp. 1–6.
25. Li, S.; Sun, Y.; Shi, W. Capacity of Magnetic-Induction MIMO Communication for Wireless Underground Sensor Networks. *Int. J. Distrib. Sens. Netw.* **2015**, *11*, 426324. [CrossRef]
26. Khalil, R.A.; Saeed, N. Optimal Relay Placement in Magnetic Induction-Based Internet of Underwater Things. *IEEE Sens. J.* **2021**, *21*, 821–828. [CrossRef]
27. Trang, H.T.H.; Dung, L.T.; Hwang, S.O. Connectivity analysis of underground sensors in wireless underground sensor networks. *Ad Hoc Netw.* **2018**, *71*, 104–116. [CrossRef]
28. Ma, H.; Liu, E.; Wang, R.; Yin, X.; Xu, Z.; Qu, X.; Li, B. Antenna Optimization for Decode-and-Forward Relay in Magnetic Induction Communications. *IEEE Trans. Veh. Technol.* **2020**, *69*, 3449–3453. [CrossRef]
29. Kisseleff, S.; Akyildiz, I.F.; Gerstacker, W. Transmitter-side channel estimation in magnetic induction based communication systems. In Proceedings of the 2014 IEEE International Black Sea Conference on Communications and Networking (BlackSeaCom), Odessa, Ukraine, 27–30 May 2014; pp. 16–21.
30. Kisseleff, S.; Akyildiz, I.F.; Gerstacker, W.H. Digital Signal Transmission in Magnetic Induction Based Wireless Underground Sensor Networks. *IEEE Trans. Commun.* **2015**, *63*, 2300–2311. [CrossRef]
31. Guo, H.; Ofori, A.A. The Internet of Things in Extreme Environments Using Low-Power Long-Range Near Field Communication. *IEEE Internet Things Mag.* **2021**, *4*, 34–38. [CrossRef]
32. Chapman, R.; Prince, M.; Guo, H. BER Analysis and Optimization of Direct Antenna Modulation for Magnetic Induction Communication. In Proceedings of the 2021 IEEE Radio and Wireless Symposium (RWS), San Diego, CA, USA, 17–22 January 2021; pp. 105–107.
33. Magnetoinductive Waves in Attenuating Media. Scientific Reports. Available online: https://www.nature.com/articles/s41598-021-85838-7 (accessed on 29 April 2021).
34. Shibalabala, J.; Swart, T.G. Performance Analysis of Wireless Mesh Networks for Underground Mines. In Proceedings of the 2020 International Conference on Artificial Intelligence, Big Data, Computing and Data Communication Systems (icABCD), Durban, South Africa, 6–7 August 2020; pp. 1–6.
35. Simon, M.K.; Alouini, M.-S. Fading Channel Characterization and Modeling. In *Digital Communication over Fading Channels*; IEEE: New York, NY, USA, 2005; pp. 17–43. ISBN 978-0-471-71523-8.
36. Wei, D.; Soto, S.S.; Garcia, J.; Becker, A.T.; Wang, L.; Pan, M. ROV assisted magnetic induction communication field tests in underwater environments. In Proceedings of the Thirteenth ACM International Conference on Underwater Networks & Systems, Shenzhen, China, 3–5 December 2018; Association for Computing Machinery: New York, NY, USA, 2018; pp. 1–5.
37. Alghamdi, R.; Saeed, N.; Dahrouj, H.; Alouini, M.; Al-Naffouri, T.Y. Towards Ultra-Reliable Low-Latency Underwater Optical Wireless Communications. In Proceedings of the 2019 IEEE 90th Vehicular Technology Conference (VTC2019-Fall), Honolulu, HI, USA, 22–25 September 2019; pp. 1–6.
38. Tonguz, O.K.; Ferrari, G. *Ad Hoc Wireless Networks: A Communication-Theoretic Perspective*, 1st ed.; Wiley: Chichester, UK; Hoboken, NJ, USA, 2006; ISBN 978-0-470-09110-4.
39. Belbase, K.; Tellambura, C.; Jiang, H. Coverage, Capacity, and Error Rate Analysis of Multi-Hop Millimeter-Wave Decode and Forward Relaying. *IEEE Access* **2019**, *7*, 69638–69656. [CrossRef]

40. Elements of Information Theory, 2nd Edition. Wiley. Available online: https://www.wiley.com/en-us/Elements+of+Information+Theory%2C+2nd+Edition-p-9780471241959 (accessed on 11 April 2021).
41. The Multinomial Theorem—Mathonline. Available online: http://mathonline.wikidot.com/the-multinomial-theorem#toc0 (accessed on 17 November 2020).